

## Integrated process of large-scale and size-controlled SnO<sub>2</sub> nanoparticles by hydrothermal method

Xue CAO, Yong-chun SHU, Yong-neng HU, Guang-ping LI, Chang LIU

Key Laboratory of Weak-Light Nonlinear Photonics, Ministry of Education,  
School of Teda Applied Physics, Nankai University, Tianjin 300457, China

Received 8 February 2012; accepted 10 April 2012

**Abstract:** SnO<sub>2</sub> nanoparticles with the average particle size of 5–30 nm were synthesized using SnCl<sub>4</sub>·5H<sub>2</sub>O as the precursor and NH<sub>3</sub>·H<sub>2</sub>O as the mineralizing agent by hydrothermal method. In the case of 1 kg/batch production, the effects of synthesis conditions including solution concentration, reaction temperature, pressure, time and pH value on the grain size, particle morphology and crystal structure of SnO<sub>2</sub> were systematically studied. The particles were characterized by X-ray diffraction (XRD) and transmission electron microscopy (TEM). The results show that, the particle size can be well controlled in the range of 5–30 nm by adjusting the processing parameters such as reaction temperature and time when the crystal structure and particle morphology remain unchanged. The previous reports, the unusual dependences of the grain size of SnO<sub>2</sub> on reaction temperature and time were found. The mechanism for such abnormal grain growth behavior was tentatively elucidated.

**Key words:** SnO<sub>2</sub>; nanoparticles; hydrothermal method

### 1 Introduction

Tin dioxide (SnO<sub>2</sub>) has long been recognized as an important n-type semiconductor. The large bandgap (3.6 eV at 300 K) and high achievable carrier concentration (up to  $6 \times 10^{20} \text{ cm}^{-3}$ ) [1] make it an excellent candidate for a wide range of application such as lithium-ion batteries, transparent conducting electrodes, and solar cells [2–4]. Recently, it is shown that small particle size and large specific surface area are essential to high performance of SnO<sub>2</sub> for applications as gas sensors and catalysts [5–7]. Therefore, considerable efforts have been focused on the synthesis of SnO<sub>2</sub> nanoparticles and the exploration of their novel properties. Various synthesis methods have been reported to prepare SnO<sub>2</sub> nanoparticles including sol-gel [8–11], chemical precipitation [12,13], hydrothermal [14–16] and microemulsion [17–19]. Among these methods, hydrothermal synthesis is often used due to its simple processes and equipment, without high-temperature sintering, allowing the control of the grain size, morphology and degree of crystallinity by easy changes in the experimental procedure. Up to now,

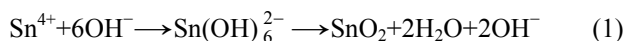
studies on the hydrothermal synthesis of SnO<sub>2</sub> have mainly focused on the exploitation of the novel morphology and crystal structure as well as flexible refinement approach. Comparatively, little work has been done on the optimization of the synthesis conditions and the practical process for large-scale synthesis.

In the present work, large-scale and size-controlled SnO<sub>2</sub> nanoparticles were prepared by the hydrolysis of SnCl<sub>4</sub>·5H<sub>2</sub>O with aqueous ammonia followed by drying. In the case of 1 kg/batch production, the processing parameter effects (solution concentration, reaction temperature, pressure, time and pH value) on particle characteristics were systematically investigated. In contrast to the previous reports, the abnormal dependences of the grain size of SnO<sub>2</sub> on reaction temperature and time were obtained. The mechanism underlying this result was tentatively exploited.

### 2 Experimental

The nano-sized SnO<sub>2</sub> powders were prepared by the conventional hydrothermal method with SnCl<sub>4</sub>·5H<sub>2</sub>O (AR) as the starting material and NH<sub>3</sub>·H<sub>2</sub>O (25%, AR) as

the mineralizing agent according to the following reaction:



The concentrations of  $\text{SnCl}_4$  were 0.5, 1.0, 1.5 and 2.0 mol/L, respectively. The terminate pH value of solutions was adjusted to 8–10 by the addition of  $\text{NH}_3 \cdot \text{H}_2\text{O}$ . The powders were then transferred to an autoclave and heated at different temperatures (160–240 °C) for different time (4–24 h). After cooling, the product was filtered, washed, and dried at 80 °C for 24 h.

The microstructure of the powder sample was characterized by transmission electron microscopy (TEM) with a JOEL–2000FX instrument. The crystal structure and phase of  $\text{SnO}_2$  were characterized by X-ray diffraction (XRD), which was carried out on all the samples with a Bruker D8 X-ray diffractometer using  $\text{Cu K}\alpha_1$  (0.15406 nm) radiation and a quartz monochromator in the  $2\theta$  range of  $10^\circ$ – $80^\circ$  in steps of  $0.02^\circ$ . The grain size was estimated with Scherrer formula [20].

In terms of different diffraction peak profiles, there are two correction methods:

1) Diffraction peak shape is similar to Cauchy function:

$$\begin{cases} f(x) = \frac{1}{1+k^2x^2} \\ \beta_{hkl} = \beta_{hkl} - b_{hkl} \end{cases} \quad (2)$$

2) Diffraction peak shape is similar to Gauss curve:

$$\begin{cases} f(x) = \exp(-k^2x^2) \\ \beta_{hkl} = \sqrt{B_{hkl}^2 - b_{hkl}^2} \end{cases} \quad (3)$$

where  $\beta_{hkl}$  is the full width at half maximum (FWHM) caused by the grain refinement in  $hkl$  diffraction direction,  $B_{hkl}$  is the FWHM of measurement, and  $b_{hkl}$  is the FWHM of instrumental broadening. In practice, the two correction methods produce very similar results. The second correction method was used in this work.

### 3 Results and discussion

#### 3.1 Effect of reaction temperature

Figure 1 shows XRD patterns for the  $\text{SnO}_2$  samples prepared at different hydrothermal temperatures ranging from 160 to 240 °C for 4 h, herein the  $\text{SnCl}_4$  solutions were all prepared at a fixed concentration of 1.5 mol/L. In each XRD pattern, the  $\text{SnO}_2$  powders are crystalline with the tetragonal rutile structure. The diffraction peaks

around  $26.6^\circ$ ,  $33.9^\circ$ ,  $37.9^\circ$ ,  $51.9^\circ$ ,  $54.8^\circ$ ,  $61.7^\circ$  and  $64.9^\circ$  are assigned to  $\text{SnO}_2$  (110), (101), (200), (211), (220), (310) and (112) (PDF No.411445), respectively. No diffraction peaks due to metallic Sn or other tin oxides are discerned. The diffraction peaks in the XRD pattern broadened due to the too small particles in the sample.

Figure 2 presents the dependence of the mean grain size of  $\text{SnO}_2$  and the maximum internal pressure on the hydrothermal temperature. The mean particle size, estimated from XRD results (Fig. 1) using Scherrer formula, increases from 10 to 18.5 nm with the increase of hydrothermal temperature. Meanwhile, the maximum internal pressure varies from 3.1 to 4.6 MPa within this temperature range. It is believed that the elevated temperature and pressure applied in the autoclave not only provide the driving force and energy for the grain growth, but also facilitate the dissolution of small particles, which can be explained by the Ostwald ripening mechanism [21].

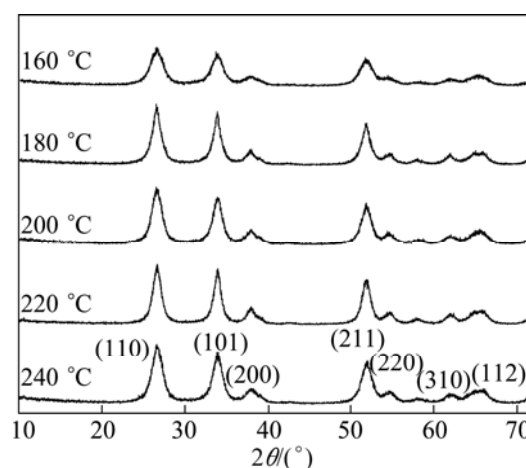


**Fig. 1** XRD patterns of  $\text{SnO}_2$  nanoparticles prepared at different hydrothermal temperatures ranging from 160 °C to 240 °C for 4 h

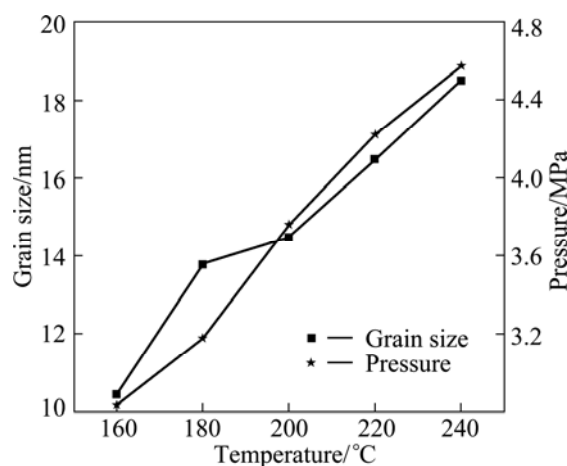


**Fig. 2** Dependence of mean grain size of  $\text{SnO}_2$  and maximum internal pressure on hydrothermal temperature

### 3.2 Effect of reaction temperature at constant pressure

In the previous study, the dependence of the crystal structure and grain size on the reaction temperature was investigated. It should be noticed that the internal pressure therein changes with the increase of the temperature since the total solution volume remains constant. Furthermore, it is also under the same conditions in the following experiments when the influence of other synthesis parameters on the particle properties is investigated.

In order to better clarify the effect of reaction temperature, the reaction was also carried out at constant pressure with varied total solution volume in this section. For comparison, reaction conditions were the same as those in section 3.1. The XRD patterns of SnO<sub>2</sub> nanoparticles at different hydrothermal temperatures and constant pressure were investigated (Figures are not shown). It can be seen that all the samples exhibit similar XRD profiles to those in Fig. 1, indicating the same crystal structure of SnO<sub>2</sub>. Figure 3 illustrates the dependence of the mean grain size of SnO<sub>2</sub> on hydrothermal temperature at a constant pressure of 4.0 MPa. Different from the results in Fig. 2, the grain size firstly increases with increasing the temperature (200–220 °C) and then decreases with further increase of temperature. The grain growth of SnO<sub>2</sub> is influenced by the nucleation rate and driving force together. The formation of tiny crystalline nuclei in a supersaturated medium occurs at first. The larger particles grow at the cost of the small particles; the reduction in surface energy is the primary driving force for the crystal growth and morphology evolution [21]. As the reaction continues, the grain sizes of SnO<sub>2</sub> decrease rapidly and the nucleation rate is significantly improved. The mechanism for the unusual decrease of the grain size

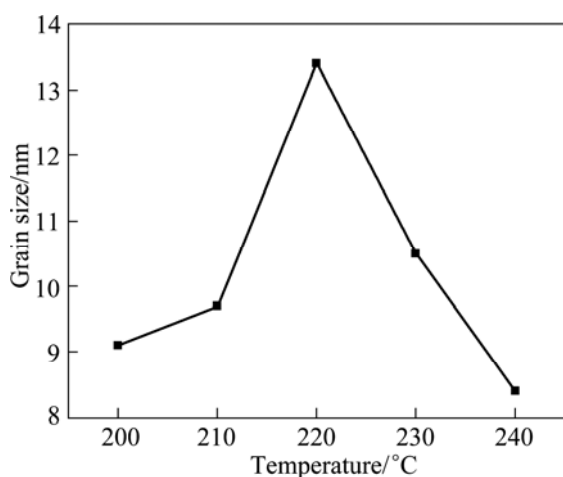


**Fig. 3** Dependence of mean grain size of SnO<sub>2</sub> on hydrothermal temperature at constant pressure of 4.0 MPa

with increasing temperature needs to be further elucidated. The abnormal grain growth is tentatively attributed to the significantly improved nucleation rate at higher temperature.

### 3.3 Effect of reaction time

For the sake of studying the effect of reaction time, various periods of the hydrothermal time were employed during the synthesis of SnO<sub>2</sub> particles. Similar to the aforementioned results, the XRD patterns (Figures are not shown) reveal that the as-grown products prepared under this condition are crystalline and possess tetragonal rutile structure. The dependence of the mean grain size of SnO<sub>2</sub> on the hydrothermal reaction periods is illustrated in Fig. 4. The grain size initially increases with rising reaction time, reaches its maximum at 12 h, and then begins to decline after prolonging reaction time. The strange behavior characteristic of a decrease in the grain size with increasing reaction time has been scarcely reported. A tentative explanation is proposed in this work as follows: at sufficiently high temperature and pressure, SnO<sub>2</sub> particles begin to nucleate and grow up with the rising reaction time. The reaction (1) is positive at this moment. When the sizes reach 15.5 nm, larger particles begin to dissolve; the reaction process becomes negative, leading to the decrease of grain sizes.

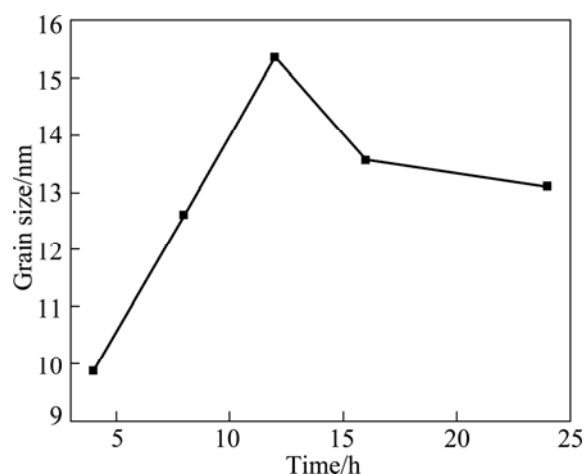


**Fig. 4** Dependence of mean grain size of SnO<sub>2</sub> on hydrothermal reaction period

### 3.4 Effect of pH value of solution

Besides reaction temperature and time, the pH value of solution is also found to be a critical parameter for the hydrothermal synthesis process. In the following experiment, SnO<sub>2</sub> particles were prepared at different pH values ranging from 8.0 to 9.5 at 200 °C for 4 h. The XRD results indicate that the tetragonal rutile structure of SnO<sub>2</sub> remains unchanged with varying pH values. The

pH value dependence of the particle size and maximum internal pressure is shown in Fig. 5. It can be seen that the particle size decreases with increasing pH value, while the maximum internal pressure varies in the contrary trend. Thus, the particle size can be controlled from about 14.5 to 10 nm by modifying the pH value of the precursor solution from 8.0 to 9.5. Combining with the results of section 3.1, increasing  $\text{NH}_4^+$  depresses the Ostwald ripening during the process of small particle dissolution. Therefore, with the increase of pH value of reaction system, the trend of grain size maintain refined.

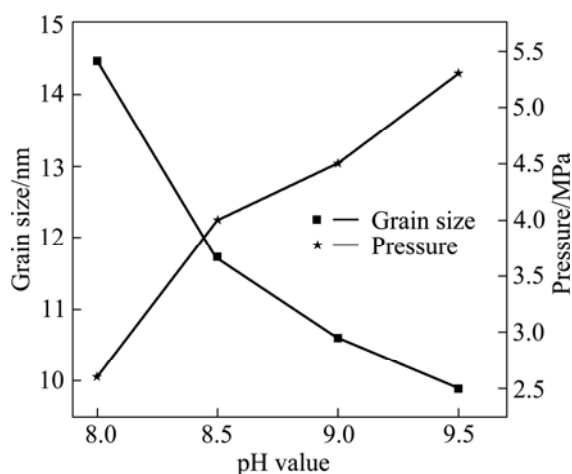


**Fig. 5** Dependence of mean grain size of  $\text{SnO}_2$  and maximum internal pressure on pH value

### 3.5 Effect of solution concentration

It is found from XRD patterns that all samples exhibit the tetragonal rutile structure (Figures are not shown). At a fixed reaction temperature, reaction time, and pH value, the mean grain size is found to depend on the solution concentration. Figure 6 shows the mean

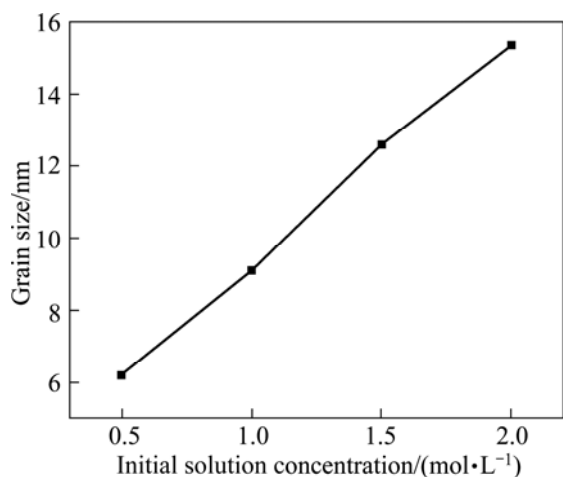


**Fig. 6** Dependence of mean grain size of  $\text{SnO}_2$  on initial solution concentration

grain sizes of  $\text{SnO}_2$  particles from different concentration solutions ranging from 0.5 to 2.0 mol/L. It can be seen from Fig. 6 that with increasing the concentration solution, the particles grow up from 6 to 16 nm. The experimental results indicate that the particle size is sensitive to the solution concentration. The control of the  $\text{SnO}_2$  particle size can be realized simply by varying the concentration of solution in the reaction system. The mass per unit volume has a 4-fold increase from 0.5 to 2.0 mol, while the single-particle mass has a 15-fold increase as the relationship between the single-particle mass  $m$  and particle size  $d$  is  $m \propto d^3$ , which indicates that increasing the solution concentration promotes the short range migration of substances and grain growth.

### 3.6 Morphologies of $\text{SnO}_2$ nanoparticles under different synthesis conditions

It is now well established that different particle morphologies of nano- $\text{SnO}_2$ , e.g., nanotube, nanobelt, and nanorod [22–25], can be obtained under different synthesis conditions. Whether the morphologies of  $\text{SnO}_2$  nanoparticles change with the synthesis conditions in this experiment needs to be essentially clarified. The results in Fig. 7 show the morphologies of  $\text{SnO}_2$  nanoparticles prepared under different synthesis conditions: initial solution concentration 0.5–2 mol/L, reaction temperature 160–240 °C, time 4–24 h, pressure 2.5–5.0 MPa and pH value 8–9.5. It can be seen that the particles are monodisperse and of quite narrow size distribution. All the samples prepared under different synthesis conditions possess similar particle size, size distribution, and morphology. In combination with the characterization results of crystal structure and grain size as described above, it might be safe to claim that size-controllable  $\text{SnO}_2$  nanoparticles in the range of 5–30 nm preserving the same crystal structure and morphology were produced by adjusting the synthesis conditions by hydrothermal method.

## 4 Conclusions

- 1) Large-scale and size-controlled  $\text{SnO}_2$  nanoparticles are obtained by the conventional hydrothermal method.
- 2) All samples exhibit the pure tetragonal rutile structure, and the particles possess similar particle size, size distribution, and morphology. By varying the experimental conditions, the particle size can be readily controlled from 5 to 30 nm.
- 3) Possible mechanism is proposed for the unusual dependences of the grain size on reaction temperature and time observed in the experiment.

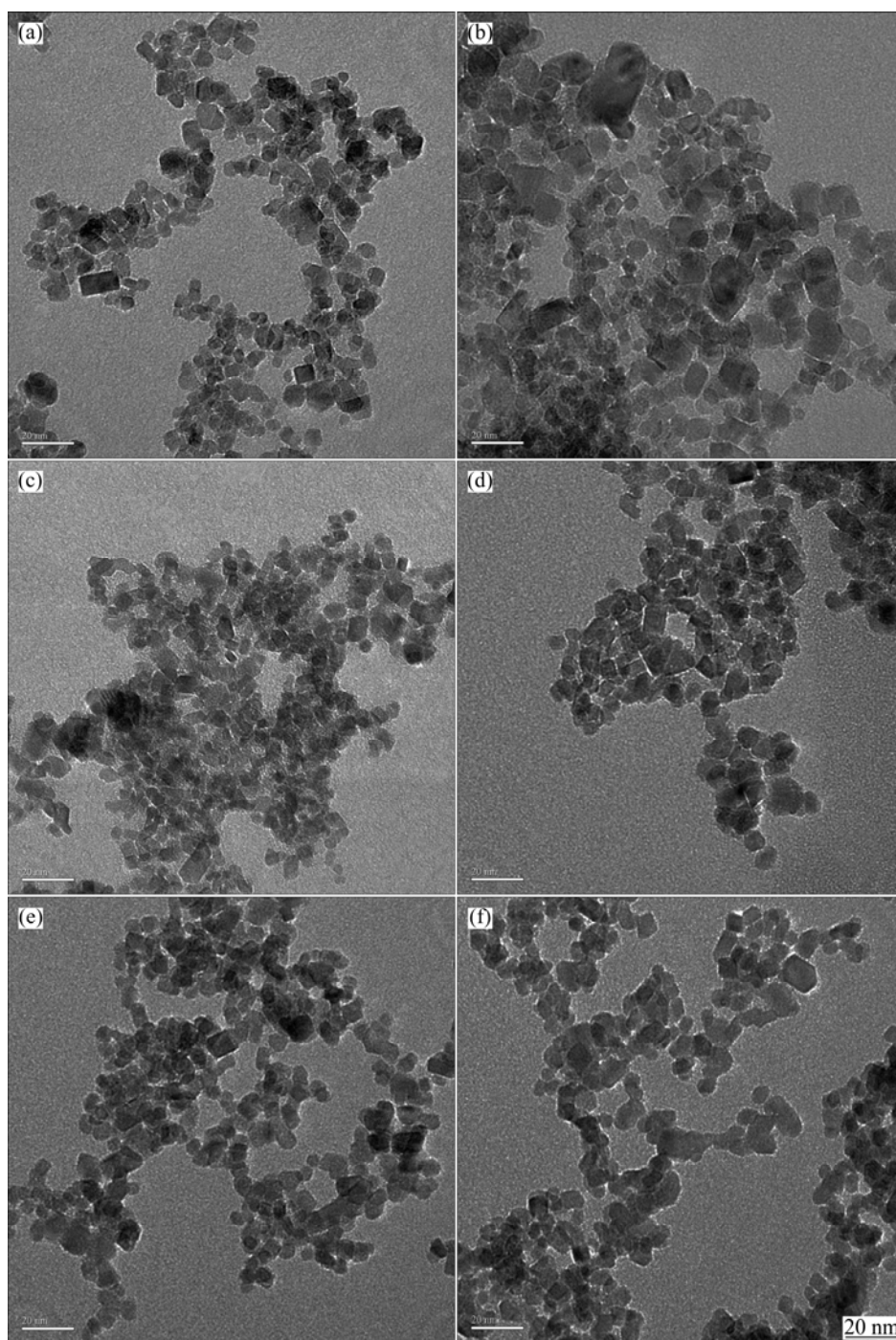


**Fig. 7** TEM micrographs of SnO<sub>2</sub> nanoparticles prepared under different synthesis conditions: (a) 1 mol/L, 200 °C, 8 h, pH9.5; (b) 1.5 mol/L, 200 °C, 8 h, pH9.5; (c) 1.5 mol/L, 200 °C, 4 h, pH9.5; (d) 1.5 mol/L, 200 °C, 4 h, pH10; (e) 1.5 mol/L, 200 °C, 4 h, pH9.0; (f) 1.5 mol/L, 220 °C, 4 h, pH9.0

## References

- [1] GROSSE P, SCHMITTE F J, FRANK G, KOSTLIN H. Preparation and growth of SnO<sub>2</sub> thin films and their optical and electrical properties [J]. *Thin Solid Films*, 1982, 90: 309–315.
- [2] PENG Zuo-yan, SHI Zhong, LIU Mei-lin. Mesoporous Sn-TiO<sub>2</sub> composite electrodes for lithium batteries [J]. *Chem Commun*, 2000, 21: 2125–2126.
- [3] FERRERE S, ZABAN A, GREGG B A. Dye sensitization of nanocrystalline tin oxide by perylene derivatives [J]. *J Phys Chem B*, 1997, 101: 4490–4493.
- [4] HE Y S, CAMPBELL J C, MURPHY R C, ARENDT M F, SWINNEA J S. Electrical and optical characterization of Sb:SnO<sub>2</sub> [J]. *J Mater Res*, 1993, 8: 3131–3134.
- [5] SBERVEGLIERI G. Classical and novel techniques for the preparation of SnO<sub>2</sub> thin-film gas sensors [J]. *Sens Actuators B: Chem*, 1992, 6: 239–247.
- [6] DIEGUEZ A, RODRIGUEZ A R, MORANTE J R. Morphological

- analysis of nanocrystalline SnO<sub>2</sub> for gas sensor applications [J]. Sens Actuators B, 1996, 31: 1–8.
- [7] YE Qing, WANG Juan, ZHAO Jian-sheng, YAN Li-na, CHENG Shui-yuan, KANG Tian-fang, DAI Hong-xing. Pt or Pd-doped Au/SnO<sub>2</sub> catalysts: High activity for low-temperature CO oxidation [J]. Catal Lett, 2010, 138: 56–61.
- [8] SHEK C H, LAI J K L, LIN G M. Grain growth in nanocrystalline SnO<sub>2</sub> prepared by sol-gel route [J]. Nanostructured Materials, 1999, 11(7): 887–893.
- [9] SHIOMI H, KAKIMOTO C, NAKAHIRA A. Preparation of SnO<sub>2</sub> monolithic gel by sol-gel method [J]. J Sol-Gel Sci Tech, 2000, 19: 759–763.
- [10] WANG Jin, LI Dun-fang, GUAN Hong-tao. Preparation of nano tin oxide powder with supersonic wave-colloidal-gel process [J]. Yunnan Metallurgy, 2002, 31(4): 42–44. (in Chinese)
- [11] GU Feng-cai, ZHAO Zhu-xuan, LI Ying-hui, MEN Juan, YAN Ju-ming, LIU Rui-xian, ZHANG Li-hua. Preparation and characterization of surface-modified SnO<sub>2</sub> nanocrystals [J]. Acta Phys Chim Sin, 2003, 19(7): 621–625. (in Chinese)
- [12] SONG K C, KANG Y. Preparation of high surface area tin oxide powders by a homogeneous precipitation method [J]. Mater Lett, 2000, 42: 283–289.
- [13] ACARBAS O, SUVACI E, DOGAN A. Preparation of nanosized tin oxide (SnO<sub>2</sub>) powder by homogeneous precipitation [J]. Ceramics International, 2007, 33: 537–542.
- [14] YANG You-ping, ZHANG Ping-min, ZHANG Yong-long, SANG Shang-bin. Preparation of uniform ultrafine SnO<sub>2</sub> powder by hydrothermal method [J]. Copper Engineering, 2004(4): 23–25. (in Chinese)
- [15] WANG Dong-xin, ZHONG Jing-ming, SUN Ben-shuang, BAO X, ZHANG Jian-rong. Tin oxide nanoparticles with controlled morphology and particle size by hydrothermal method [J]. Chinese Journal of Inorganic Chemistry, 2008, 24(6): 892–896. (in Chinese)
- [16] PIRES F I, JOANNI E, SAVU R, ZAGHETE M A, LONGO E, VARELA J A. Microwave-assisted hydrothermal synthesis of nanocrystalline SnO powders [J]. Materials Letters, 2008, 62: 239–242.
- [17] PAN Qing-yi, XU Jia-qiang, LIU Hong-min, AN Chun-xian, JIA Na. Preparation microstructure and gas sensing properties of nanosized SnO<sub>2</sub> materials made by microemulsions [J]. J Inorg Mater, 1999, 14(1): 83–89. (in Chinese)
- [18] SONG K C, KIM J H. Preparation of nanosize tin oxide particles from water-in-oil microemulsions [J]. J Colloid Interf Sci, 1999, 212: 193–196.
- [19] SONG K C, KIM J H. Synthesis of high surface area tin oxide powders via water-in-oil microemulsions [J]. Powder Technology, 2000, 107: 268–272.
- [20] GUO Jin-ling, SHEN Yue-nian. Several issues in calculation of grain size with Scherrer formula [J]. Journal of Inner Mongolia Normal University: Natural Science Edition, 2009, 38(3): 357–358. (in Chinese)
- [21] FAN Wei-liu, ZHAO Wei, YOU Li-ping, SONG Xin-yu, ZHANG Wei-min, YU Hai-yun, SUN Si-xiu. A simple method to synthesize single-crystalline lanthanide orthovanadate nanorods [J]. J Sol Stat Chem, 2004, 177: 4399–4403.
- [22] LIU Ying, LIU Mei-lin. Growth of aligned square-shaped SnO<sub>2</sub> tube arrays [J]. Adv Funct Mater, 2005, 15(1): 57–62.
- [23] FAGLIA G, BARATTO C, SBERVEGLIERI G. Adsorption effects of NO<sub>2</sub> at ppm level on visible photoluminescence response of SnO<sub>2</sub> nanobelts [J]. Applied Physics Letters, 2005, 86: 11923–11926.
- [24] HOU De-dong, LIU Yin-kai. Synthesis and characterization of SnO<sub>2</sub> nanorods [J]. J Inorg Mater, 2002, 17(4): 691–694.
- [25] CHENG Bin, RUSSELL J M, SHI Wen-sheng, ZHANG Lei, SAMULSKI E T. Large-scale, solution-phase growth of single-crystalline SnO<sub>2</sub> nanorods [J]. J Am Chem Soc, 2004, 126(19): 5972–5973.

## 水热法批量制备粒径可控 SnO<sub>2</sub> 纳米粉体

曹雪, 舒永春, 胡永能, 李广平, 刘畅

南开大学 泰达应用物理学院 弱光非线性光子学材料教育部重点实验室, 天津 300457

**摘要:** 以 SnCl<sub>4</sub>·5H<sub>2</sub>O 为前驱体、NH<sub>3</sub>·H<sub>2</sub>O 为矿化剂, 通过水热还原技术制备平均粒径在 5~30 nm 的 SnO<sub>2</sub> 纳米粉末。系统研究小批量生产(1 kg/批)条件下, 工艺条件包括溶液浓度、反应温度、压力、时间和 pH 值对 SnO<sub>2</sub> 粒径、形貌和晶型的影响, 并采用 XRD、TEM 等测试手段对样品进行表征。结果表明, 在保持 SnO<sub>2</sub> 粉末晶型和形貌不变的前提下, 通过调节反应温度、反应时间等工艺参数, 粉末的粒径尺寸可以有效地控制在 5~30 nm 范围内。不同于之前的报道, SnO<sub>2</sub> 粒径尺寸随着反应时间(反应温度)的变化存在新的变化趋势, 并推测解释了此晶粒异常生长的机理。

**关键词:** SnO<sub>2</sub>; 纳米粉末; 水热法

(Edited by Wei-ping CHEN)